JOURNAL OF Applied Polymer SCIENCE

Synthesis and Properties of P(NIPAAm-*co*-AM)/SiO_2 Hybrid Temperature-Sensitive Hydrogels

Yun-Long Li,[1,2] Na Ouyang,[1,2] Ai-Ru Ke,[1,2] Song-Bai Lin[1,2]

[1]Department of Light-Textile Engineering, Liming Vocational University, Quanzhou 362000, Fujian, China

[2]Applied Technology Engineering Center of Fujian Provinicial High Education for Practical Chemical Material, Fujian 362000, China

Correspondence to: Y.-L. Li (E-mail: ylli@lmu.edu.cn)

ABSTRACT: Using *N, N′*-methylene bisacrylamide as crosslinking agent and potassium peroxydisulfate as initiator, the temperature-sensitive hydrogels were prepared with organic monomer *N*-isopropylacrylamide (NIPAAm) and acrylic amide and inorganic material ethyl orthosilicate (TEOS). The structure of hybrid hydrogels was represented by scanning electron microscopy and Fourier transform infrared spectroscopy. The volume phase transition temperature (VPTT) of hybrid hydrogels was determined by differential scanning calorimetry thermograms of the swollen hydrogel. The results showed that the VPTT of the hydrogels increased with the increasing of TEOS dosage. When the temperature was lower than VPTT, the hydrogels exhibited excellent temperature sensitivity and kept at a swelling state, but when the temperature was higher than VPTT, the hydrogels deswelled significantly. In addition, the compressive strength of hydrogels was studied, the results showed that hybrid hydrogels had more ideal mechanical properties than organic hydrogels. © 2012 Wiley Periodicals, Inc. J. Appl. Polym. Sci. 000: 000–000, 2012

KEYWORDS: hydrogels; temperature sensitivity; volume phase transition; silica

Received 26 February 2012; accepted 3 June 2012; published online

DOI: 10.1002/app.38146

INTRODUCTION

Based on their reversible responsiveness in response to environmental stimuli, intelligent hydrogels have an attractive prospect of application in numerous fields including controlled release, chemical transducer, artificial muscles, nanodevice, drug delivery, and intelligent separation.[1–5] According to different stimuli, intelligent hydrogels can be divided into temperature-sensitive, pH-sensitive, electric field sensitive, light-sensitive, magnetic field sensitive, biomolecule-sensitive hydrogels, and so forth.[6,7] Temperature-sensitive hydrogels exhibit a volume phase transition at a lower critical solution temperature (LCST), whose volume can shrink with rising or lowering temperature.[8–10] Poly(*N*-isopropylacrylamide) (PNIPAAm) hydrogel is the most frequently investigated temperature-sensitive polymer, which shows shrinkage in volume once the temperature is raised above the LCST and dissolves at low temperatures because of its obvious hydrophilic and hydrophobic changes in small temperature range.[11] Inomata,[12] Hiroki,[13] and Bae[14] synthesized hydrogels based on different N-substituted acrylamides and researched temperature-sensitive mechanism.

Recently, the temperature-sensitive hydrogel is prepared with organic polymers, and this kind of hydrogel has common weakness in low intensity. Because the sensitivity is generated by synergistic reaction between hydrophilic group and hydrophobic group, phase separation appears inside the hydrogels, which leads to break hydrogels under the effect of internal stress. This drawback limits their application on biological machinery and membrane separation system in a large extent. It is a problem needed to be resolved that hydrogels of high strength are prepared without interrupting the original temperature sensitivity. We have discussed this problem through several ways.[15–18] Preparation of the hybrid intelligent hydrogels by adding inorganics into hydrogels is one of the ideal means.

P(NIPAAm-*co*-AM)/SiO_2 hydrogels were prepared by *in situ*-gel solution polymerization with *N*-isopropylacrylamide (NIPAAm) and acrylic amide (AM) as organic monomer and ethyl orthosilicate (TEOS) as precursor. The structure of the hydrogels was characterized by scanning electron microscopy (SEM) and Fourier transform infrared (FTIR) spectroscopy. The sensitivity and stress strength of the hybrid hydrogels were also studied.

EXPERIMENTAL

Materials

AM, *N, N′*-methylene bisacrylamide, TEOS, and concentrated hydrochloric acid (HCl) were purchased from China National Medicines Corporation (Beijing, China). NIPAAm (AR) was purchased from Shanghai Content Competition Chemical

Table I. Sample Preparation, ESR in Deionized Water

Sample code	NIPAAm (g)	AM (g)	TEOS (g)	ESR (g/g)
Gel 1	12	8	0	32.5
Gel 2	12	8	1.0	32.1
Gel 3	12	8	2.0	30.2
Gel 4	12	8	4.0	22.5

Technology Corporation (Shanghai, China). Potassium peroxydisulfate (KPS), *N, N*-dimethyl formamide, ethanol (C_2H_5OH), and sodium chloride (NaCl) were purchased from Guangdong Xilong Chemical Corporation (Guangdong China).

Synthesis of P(NIPAAm-*co*-AM)/SiO_2 Hydrogels

First of all, Specific quantities of TEOS were dissolved in pH = 3–5 HCl solution, after 2 h, silicasol was prepared. The quantities of dissolved NIPAAm in distilled water and acrylic acid were brought into the three-necked bottle. After bubbling nitrogen for 30 min, a certain amount of crosslinking agent, silicasol and initiator were added into the three-necked bottle, which was stirred in the reaction mixer for a while up to 55°C, and then translucent gel was prepared. To allow the unreacted chemicals and impurity substances to leach out from the hydrogel, the hydrogel was immersed in distilled water for 7 days, and the distilled water must be replaced at intervals. We got pure P(NIPAAm-*co*-AM)/SiO_2 hydrogels after drying. The detailed feed compositions are listed in Table I.

FTIR Analysis of Hydrogels

The samples were measured using FTIR spectroscopy (USA Nicolet Magna-IR 750 spectrometer) after pressing the disk of KBr and samples.

Surface Morphology Analysis of Hydrogels

After the cross-section of hydrogels coated with gold, surface morphology was measured using Germany LEO-1530 SEM.

Swelling Behavior of Hydrogels

Measurement of Equilibrium Swelling Ratio. Hydrogel sample was immersed in deionized water at 25°C until reaching the equilibrium state, then the equilibrium swelling ratio (ESR) was calculated as follows:

$$\mathrm{ESR} = (W_e - W_d)/W_d \quad (1)$$

where W_e is the equilibrium weight of the swollen hydrogel and W_d is the weight of dry hydrogel.

Measurement of Swelling Kinetics. The dried hydrogels were used to determine their swelling ratio in deionized water. For calculation of the swelling ration, the following equation is used:

$$\mathrm{SR} = (W_t - W_d)/W_d \quad (2)$$

where W_t is the mass in the swollen state at certain time and W_d is the weight in dried state.

At the beginning of each experiment, W_d of a piece of hydrogels was measured by weight, and then, it was immersed in an excess of deionized water for swelling. At specified time intervals, the hydrogel was removed from the water and removed adhering water by paper tissue, then weighted to measure W_t.

Measurement of Temperature Sensitivity

Specific quantities of dry hydrogel were immersed in deionized water at different temperatures (from 20 to 50°C). When the swelling hydrogels reach equilibrium, they were taken out and weighted after removing excess water from the surface by wet filter paper. The ESR was calculated according to eq. (1).

Measurement of Volume Phase Transition Temperature

Volume phase transition temperature (VPTT) was measured using USA TA DSC-2910 differential scanning calorimetry (DSC) analyzer. Ten milligrams of hydrogels that have reached swollen equilibrium was added into sample cell. The temperature was raised from 0 to 50°C in the nitrogen atmosphere, and heating rate was 1°C/min.

Measurement of Compressive Strength

Compressive strength of the swollen hydrogel that was cut into $10 \times 10 \times 10$ mm^3 was tested using universal mechanics tester. The hydrogel was compressed by the tester at the speed of 2 mm/min until it broke. Compressive strength (Ss) was calculated as follows:

$$\mathrm{Ss} = F/S \quad (3)$$

where F is the force of cross section and S is the cross-sectional area of the sample.

RESULTS AND DISCUSSION

Structure Characterization of Hydrogels

FTIR Analysis. The infrared spectra of P(NIPAAm-*co*-AM)/SiO_2 and P(NIPAAm-*co*-AM) are shown in Figure 1(a, b). In Figure 1(b), the wide absorption bands nearby 3300 cm^{-1} could be attributed to —NH_2— and —NH—, the frequency doubling stretching vibrating peak at 3080 cm^{-1} could be attributed to the secondary strong amide band, and the characteristic bands

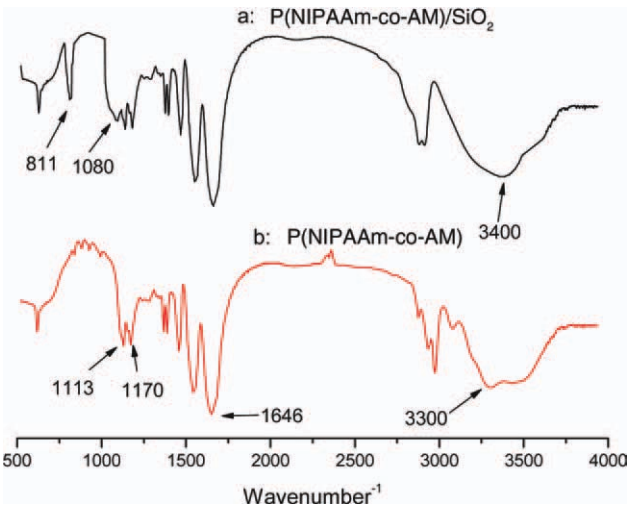

Figure 1. The FTIR spectra of the samples. a: P(NIPAAm-*co*-AM)/SiO_2 and b: P(NIPAAm-*co*-AM)). [Color figure can be viewed in the online issue, which is available at wileyonlinelibrary.com.]

at 2970, 2930, and 2875 cm^{-1} are belong to C—H stretching of methyl and methylene. The peaks at 1646 and 1455 cm^{-1} represent the carbonyl group and —CH3 asymmetric bending vibrations, respectively. The peak at 1540 cm^{-1} belongs to the N—H bend vibration. The peak at 1359 cm^{-1} depicts the characteristic vibrational peak of C—N bond. The peaks at 1170 and 1113 cm^{-1} relate to the C—C stretching vibrations of —$CH(CH_3)_2$. According to the obtained FTIR spectra from Figure 1(b), it is concluded that the structure of the P(NIPAAm-*co*-AM) hydrogel consists of a sequence of hydrophilic amide group (—$CONH_2$) and hydrophobic isopropyl (—$CH(CH_3)_2$). When the spectrum of the P(NIPAAm-*co*-AM) hydrogel is compared with the reference spectra of the P(NIPAAm-*co*-AM)/SiO_2 [see Figure 1(a)], the original peaks of C—C stretching vibrations of —$CH(CH_3)_2$ at 1170 and 1113 cm^{-1} show small displacement, and become wider. The peaks at 811 and 1080 cm^{-1} correspond to Si—O—C vibrating absorption peak and Si—O—Si bonding vibration, respectively. The peak at 3300 cm^{-1} depicts unreacted Si—OH, and this peak overlaps the peak that is related to the original broad bands of —NH_2— and —NH—, at 3300 cm^{-1} in P(NIPAAm-*co*-AM) spectrum.

Morphological Analysis by SEM. Figure 2 depicts the morphological appearance of Gel 1 [Figure 2(a)], Gel 2 [Figure 2(b)], and Gel 4 [Figure 2(c)]. It can be seen that the pure organic hydrogel [Gel 1, Figure 2(a)] appeared to be neat and morphologically homogeneous while white dot could be seen in the Gel 2 [Figure 2(b)] and Gel 4 [Figure 2(c)]. Moreover, with an increase of TEOS dosage, the white dot became denser. In the Gel 2, the white dot appeared to be small particles of nanometer size and distributed uniformly, but in the Gel 4, the white dot occurred agglomeration, and the surface appeared to phase separation. This primarily confirmed that there are some uncondensed hydroxyl group (—OH) on the surface of the hydrogel if SiO_2 was introduced into the hydrogel using TEOS as precursor. In P(NIPAAm-*co*-AM)/SiO_2, the hydrogen bonds or chemical bonds between the —OH or between the —OH and other functional group (such as —NH_2) be formed. When the dosage of TEOS is little (Gel 2), the hydrogen bonds between the —OH and other functional group play a major role, which contributed to the uniform dispersion of SiO_2 in the organic phase. But with the increasing amount of TEOS, the hydrogen bonds between the —OH became dominant, which lead to agglomeration of the SiO_2 particle, evenly, may cause obvious phase separation if the amount of TEOS is excess (Gel 4) when the hydrogen bonds between the —OH was strong.

Swelling Behavior Analysis of Hydrogels

The hydrogels with different amounts of TEOS (Gel 1, Gel 2, Gel 3, and Gel 4) were used for the swelling behavior studies. Table I shows the ESR of the hydrogels with different amounts of TEOS, and Figure 3 shows the effect of the quantity of TEOS on the swelling kinetics.

As shown in Table I, there was basically no difference between Gel 1 and Gel 2 on their swelling ratio, but addition of 4.0 g of TEOS resulted in a sharp decrease from 32.5 g/g (Gel 1) to 22.5 g/g (Gel 4). The structure of the P(NIPAAm-*co*-AM) hydrogel consists of a sequence of strong hydrophilic groups (—NH_2),

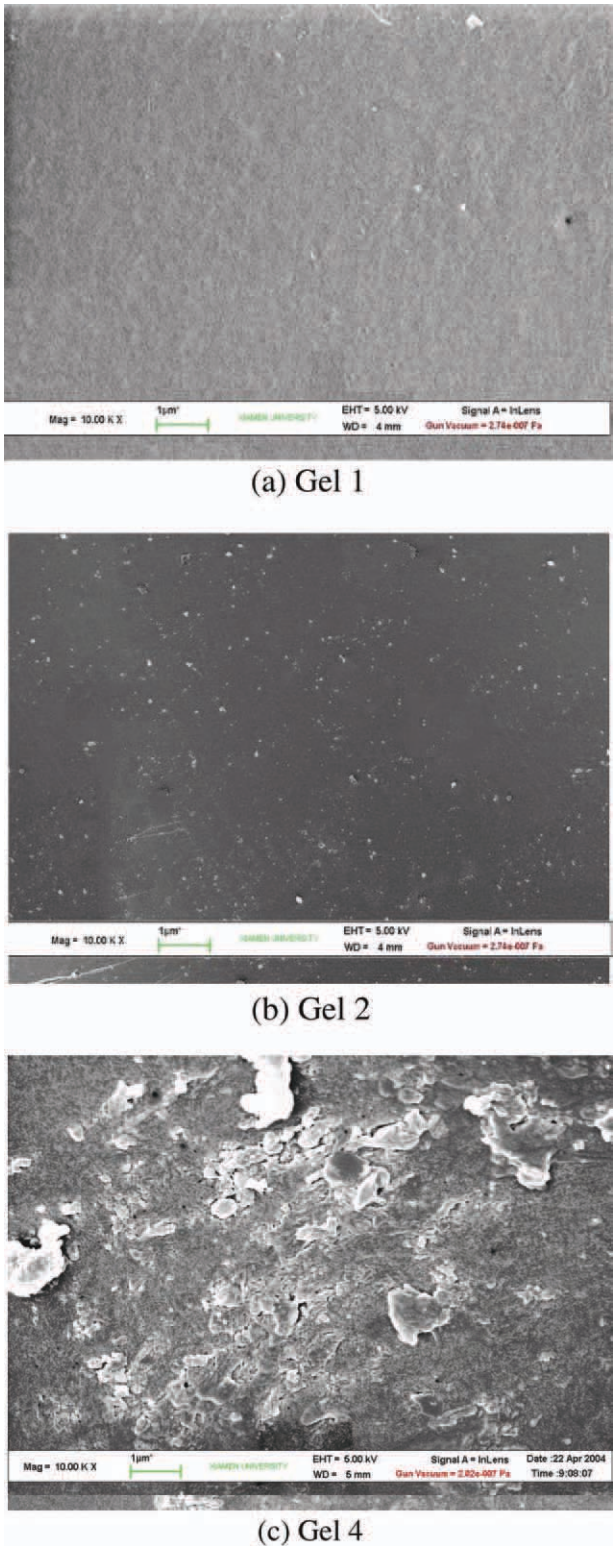

Figure 2. SEM photographs of hydrogels with different contents of TEOS (×10.00 KX). (a) Gel 1; (b) Gel 2; and (c) Gel 4. [Color figure can be viewed in the online issue, which is available at wileyonlinelibrary.com.]

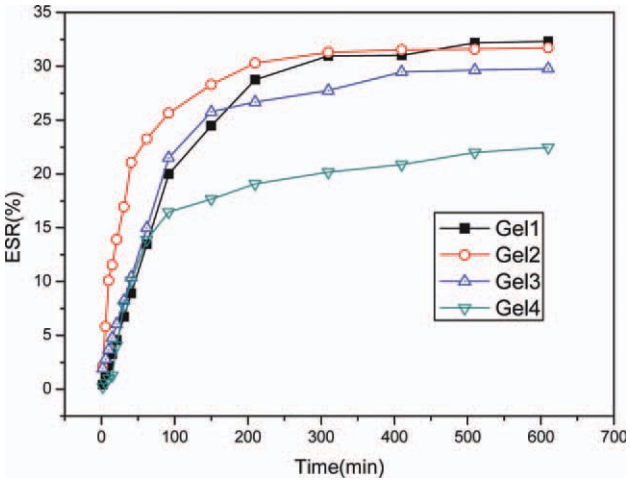

Figure 3. The swelling kinetics of hydrogels in deionized water. [Color figure can be viewed in the online issue, which is available at wileyonlinelibrary.com.]

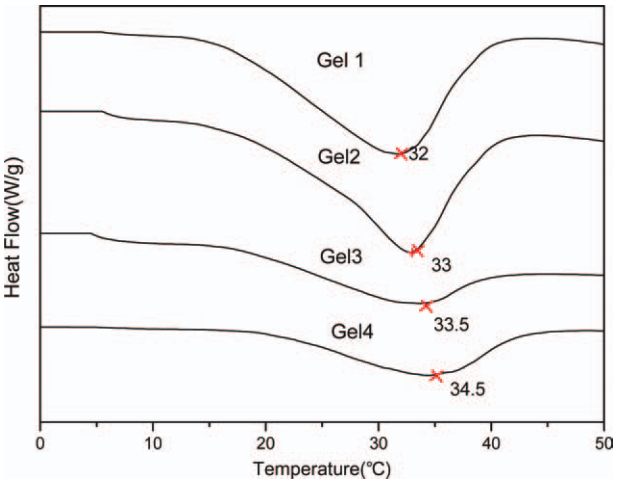

Figure 4. DSC thermograms of the swollen hydrogels. [Color figure can be viewed in the online issue, which is available at wileyonlinelibrary.com.]

and the structure of TEOS consists of a large number of uncondensed nonionic hydrophilic groups (—OH), which existed in the end of inorganic hydrogel, so the addition of TEOS would not weaken the hydrophilicity of the hydrogel. But if the amount of TEOS is excess, the SiO_2 particle may agglomerate easily and the structure may occur obvious phase separation that due to the decrease in swelling ratio (Gel 3, Gel 4).

As shown in Figure 3, the hydrogel that contain 1.0 g of TEOS (Gel2) can swell more quickly than Gel 1, Gel 3, and Gel 4, moreover, Gel 1 swell more faster than Gel 3 and Gel 4. The swelling behavior of the hydrogel depends on the effect of osmotic pressure and surface adsorption inside and outside of the network. A good organic/inorganic hybrid mechanism was formed in the structure of the hydrogel, when 1.0 g TEOS was brought into the system. This mechanism can enhance the effect of surface adsorption and penetration of the network, so the swell ration of Gel 2 is faster than that of Gel 1. But for Gel 3 and Gel 4, inorganic components agglomerated, and appeared phase separation due to the excess of TEOS will hinder the diffusion of water in the three-dimensional network of hydrogel, so the swelling rate decreases gradually.

Measurement of VPTT

Temperature-sensitive hydrogels are hydeogels that undergo large changes in the swelling ratio (such as swell shrink) by only a small variation about temperature, so during the process of volume phase transition, the temperature-sensitive hydrogels always show obvious endothermic phenomenon. The VPTT is defined as the temperature (T_{max})[19–23] corresponding to the lowest point of the endothermic peak of the hydrogel or initial temperature (T_o) occurring endothermic phenomenon. In this article, T_{max} is characterized as VPTT.

The thermal-transition behavior of the hydrogels (Gel 1, Gel 2, Gel 3, and Gel 4) were investigated using DSC. As shown in Figure 4, The apparent volume phase transition occur for Gel 1 and Gel 2, and the T_{max} of the two samples were 32 and 33°C respectively, but this phenomenon about volume phase transition was evidently weakened, even maybe disappeared, as shown in the curves of Gel 3 and Gel 4. These results correspond to the temperature sensitive theory of PNIPAAm, which showed that hybrid hydrogels with inorganic silicon could maintain the sensitivity of PNIPAAm. On the other hand, the poorer hydrophilic of P(NIPAAm-*co*-AM)/SiO_2 and better heat resistance of inorganic components contributed to increase T_{max} slightly.

Temperature Sensitivity of Hydrogels

Figure 5 shows the effect of different amounts of TEOS on temperature sensitivity. As shown in Figure 5, the hydrogels can occur volume transition at a certain temperature that was corresponding to the VPTT measured from DSC. The temperature sensitivity of the P(NIPAAm-*co*-AM)/SiO_2 (Gel 2) was similar to that of P(NIPAAm-*co*-AM) (Gel 1). On the other hand, the temperature occurring for volume transition increased as the increasing of TEOS's amount as which the temperature-

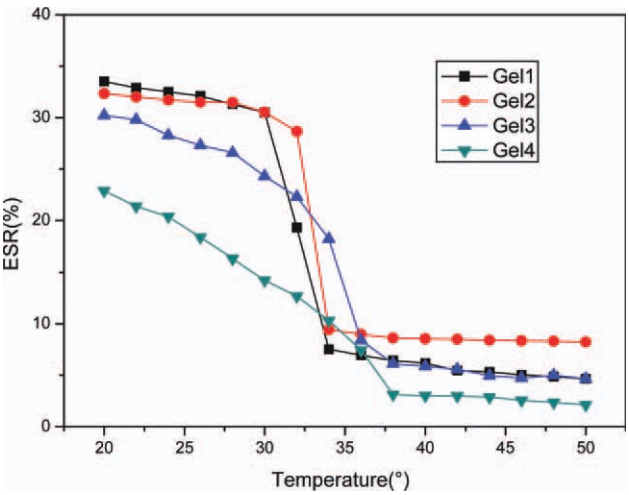

Figure 5. Temperature-responsive curves of hydrogels. [Color figure can be viewed in the online issue, which is available at wileyonlinelibrary.com.]

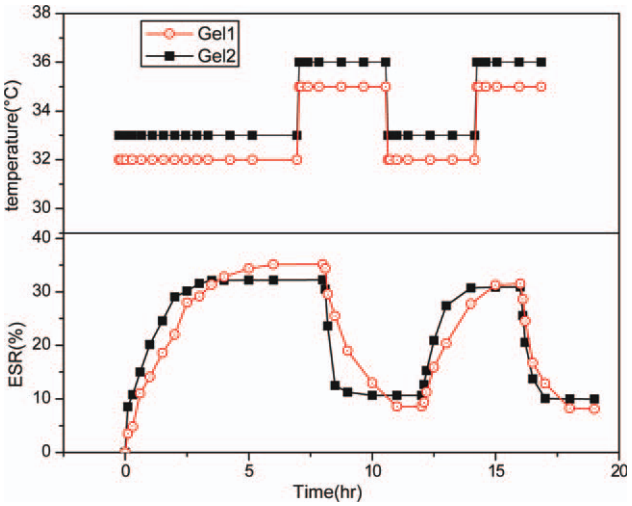

Figure 6. The temperature-stimulating swelling–deswelling kinetics of Gel 1 and Gel 2 on different temperatures. [Color figure can be viewed in the online issue, which is available at wileyonlinelibrary.com.]

sensitivity of P(NIPAAm-*co*-AM)/SiO_2 weakened and evenly disappeared. These results also correspond to that of DSC test. The VPTT increase was due to the strong hydrogen bonds formed between the inorganic silica hydrogel, P(NIPAAm-*co*-AM), and water molecules and the reinforce of heat resistance because of SiO_2. But, if the content of SiO_2 is excessive, the structure of the P(NIPAAm-*co*-AM)/SiO_2 occur phase separation, which causes the decrease of ESR, limited the fully stretch of hydrogel network. The limitation hindered the aggregation of hydrophobic groups of the hydrogen that due to reduce the temperature sensitivity.

Figure 6 depicts the dynamic swelling/deswelling behaviors of Gel 1 and Gel 2 in distilled water with different temperatures, the test temperature was 32–35°C for Gel 1 and 33–36°C for Gel 2. The dry hydrogels Gel 1 and Gel 2 were immersed in distilled water at response temperature (32 and 33°C, respectively) to reach swelling equilibrium, then moved into distilled water of higher temperature (35 and 36°C, respectively) to carry out deswelling, and so repeatedly.

As shown in Figure 6, The hydrogels Gel 1 and Gel 2 swell at 32 and 33°C, respectively, and then shrink at 35 and 36°C respectively; it is concluded that P(NIPAAm-*co*-AM) and P(NIPAAm-*co*-AM)/SiO_2 hydrogels were both heat-shrink temperature-sensitive hydrogels. On the other hand, whether the swelling process or deswelling process, response rate of hybride hydrogel was faster than P(NIPAAm-*co*-AM). This result was also consistent with the conclusion of swelling behavior. So, it is concluded that a good hybrid intelligent hydrogel could increase the response speed after introducing SiO_2. It was also found that response process can be repeated, and swelling rate always changed with changing temperature. Eighteen hours later, the swelling properties of two hydrogels showed almost no decline after repeated experiments, which showed the temperature response of the hydrogel could be repeatedly carried out.

Compressive Performance of Hydrogels

The effect of different amounts of TEOS on compressive strength about swollen hydrogen (SR is 15 g/g) was studied. As shown in Figure 7, the compressive strength of Gel 4 was the poorest because of apparent coacervation. The compressive strength of Gel 1 was 12.7 MPa, which is poorer than Gel 2 with the compressive strength about 19.5 MPa and Gel 3 with the compressive strength about 14.2 MPa. It can be concluded that SiO_2 inorganic network played a good role in enhancement of organic components, and the most ideal hybrid hydrogel Gel 2 could form a good organic/inorganic hybrid network. Inorganic silica hydrogel could play a very good role in enhancing organic network. The hydrogel (Gel 4) containing excessive amount of SiO_2 could not form a good organic/inorganic hybrid structure and enhance the effect of inorganic components, which cause a downward trend in compressive strength.

CONCLUSIONS

1. In this study, it showed that P(NIPAAm-*co*-AM)/SiO_2 hybrid hydrogel with uniform structure was successfully synthesized through this experimental scheme.
2. In the system of P(NIPAAm-*co*-AM)/SiO_2 hybrid hydrogel, ESR and swelling rate decreased with the increasing amount of TEOS, whereas ESR and swelling rate of the ideal hybrid hydrogel (Gel 1) were slightly better than P(NIPAAm-*co*-AM) hydrogel.
3. It was found that a series of hydrogels showed a clear volume phase transition behavior by DSC study, and VPTT of the hydrogel increased with the increasing amount of TEOS. If the amount of TEOS was too large, VPTT became unobvious or even disappeared.
4. By studying temperature sensitivity of hydrogels, it was found that pure organic hydrogel (Gel 1) and ideal hybrid hydrogel (Gel 2) had good temperature sensitivity. Response temperature was around 32 and 33°C, respectively. The hydrogel showed the swelling state in deionized water below VPTT and showed deswelling state in

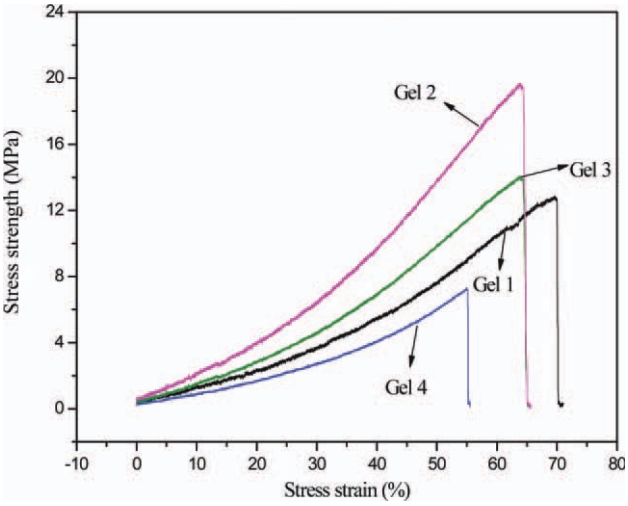

Figure 7. The stress–strain of the different hydrogels. [Color figure can be viewed in the online issue, which is available at wileyonlinelibrary.com.]

deionized water above VPTT. The response of the hydrogel could be repeated.

5. The hybrid hydrogel prepared by *in situ*-gel polymerization had good mechanical properties. The maximum compressive strength was up to 19.5 MPa, and pure organic hydrogel was only 12.7 MPa.

ACKNOWLEDGMENTS

This work was financially supported by Natural Science Foundation of Fujian Province (No. 2009J01319) and Special Personnel Training Program of Quanzhou (No. 10A01).

REFERENCES

1. Hamlen, R. P.; Kent, C. E.; Shafer, S. N. *Nature* **1965,** *206*, 1149.
2. Tanaka, T.; Nishio, Z.; Sun, S. T.; Ueno-Nishio, S. *Science* **1982,** *218*, 467.
3. Wallmersperger, T.; Kroplin, B.; Gulch, R. W. *Mech. Mater.* **2004,** *36*, 411.
4. Okano, T.; Kikuchi, A.; Sakurai, Y.; Takei, Y.; Otata, N. *J. Controlled Release* **1995,** *36*, 125.
5. Cicek, H.; Tuncel, A. *J. Polym. Sci. Part A: Polym. Chem. Ed.* **1998,** *36*, 543.
6. Supranee, K.; Siridech, B. *Eur. Polym. J.* **2006,** *42*, 1609.
7. Yin, L. C.; Zhao, Z. M.; Hu, Y. Z.; Ding, J. Y.; Cui, F. Y.; Tang, C.; Zhao, C. H. *J. Appl. Polym. Sci.* **2008,** *108*, 1238.
8. Katayama, S.; Hirokawa, Y.; Tanaka, T. *Macromolecules* **1984,** *17*, 2641.
9. Yun, J.; Kim, H. *Polym. Bull.* **2012,** *68*, 1109.
10. Kevin, J. P.; Charles, V. R. *J. Polym. Sci. Part A: Polym. Chem.* **2012,** *50*, 1374.
11. Stevin, H. G.; Maria, P.; Akhtar, M. K. *Polym. Int.* **1992,** *29*, 29.
12. Inomata, H.; Goto, Sh. Ch.; Saito, S. *Macromolecules* **1990,** *23*, 4887.
13. Takei, Y. G.; Aoki, T.; Sanui, K.; Ogata, N.; Sakurai, Y.; Okano, T. *Macromolecules* **1994,** *27*, 6163.
14. Bae, Y. H.; Okano, T.; Kim, S. W. *J. Polym. Sci. Part B: Polym. Phys.* **1990,** *28*, 923.
15. Lin, S. B.; Yuan, C. H.; Ke, A. R.; Quan, Z. L. *Sens. Actuators B: Chem.* **2008,** *134*, 281–286.
16. Yuan, C. H.; Lin, S. B.; Liu, B.; Ke, A. R.; Quan, Z. L.; Yuan, C. H.; Lin, S. B.; Liu, B.; Ke, A. R.; Quan, Z. L. *Sens. Actuators B: Chem.* **2009,** *140*, 155.
17. Li, Y. L.; Ke, A. R.; Lin, S. B.; Ouyang, N. *Int. J. Polym. Mater.* **2011,** *60*, 1164.
18. Lin, S. B.; Wu, J. H.; Yao, K. D.; Cai, K. Y.; Xiao, C. M.; Jiang, C. J. *Compos. Interfaces* **2004,** *11*, 271.
19. Koeji, M.; Vuk, A.; Jerman, I. *Sol. Energy Mater. Sol. Cells* **2009,** *93*, 1733.
20. Otake, K.; Inomata, H.; Konno, M.; Saito, S. *Macromolecules* **1990,** *23*, 283.
21. Feil, H.; Bae, Y. H.; Feijen, J.; Kim, S. W. *J. Membr. Sci.* **1991,** *64*, 283.
22. Kaneko, T.; Asoh, T.; Akashi, M. *Macromol. Chem. Phys.* **2005,** *206*, 566.
23. Singh, D. Knuckling, D. Choudhary, V. Adler, H.-J. Koul, V. *Polym. Adv. Technol.* **2006,** *17*, 186.